Applied Catalysis A: General 386 (2010) 65–73

Contents lists available at ScienceDirect

Applied Catalysis A: General

journal homepage: www.elsevier.com/locate/apcata

Diesel-length aldehydes and ketones via supercritical Fischer Tropsch Synthesis on an iron catalyst

Ed Durham, Sihe Zhang, Christopher Roberts*

Department of Chemical Engineering, Auburn University, 210 Ross Hall, AL 36849, USA

ARTICLE INFO

Article history:
Received 10 May 2010
Received in revised form 14 July 2010
Accepted 18 July 2010
Available online 22 July 2010

Keywords:
Fischer Tropsch Synthesis
Supercritical fluids
Iron catalyst
Aldehyde
Ketone
CO insertion
Mechanism

ABSTRACT

Use of an iron-based catalyst (1 Fe:0.01 Cu:0.02 K by mole with and without 0.1 Zn) for Fischer Tropsch Synthesis with a supercritical hexanes reaction media resulted in a significant selectivity towards diesel-length aldehydes and methyl-ketones. Varying the residence time indicated that aldehydes are primary products that are converted by secondary reactions to olefins. Additionally, incorporation studies showed that octyl aldehyde and octyl alcohol incorporated into growing chains while the octyl olefin did not. The results of this work support n-alkanes and aldehydes as primary products, olefins as both primary and secondary products, CH_4 and CO_2 as secondary products, and an oxygenate mechanism for propagation.

1. Introduction

Fischer Tropsch Synthesis (FTS) is a process for converting syngas ($CO + H_2$) to fuels and chemicals. FTS can be performed at high temperature (HTFT) on an iron catalyst for the production of gasoline and light olefins or at low temperature (LTFT) on either an iron or cobalt catalyst for the production of diesel and wax [1]. Iron is cheaper [1] and less active [2] than cobalt. Iron offers water–gas shift activity, allowing for a lower usage ratio (the ratio of the rate of consumption of H_2 to the rate of consumption of CO) and a broader range of the syngas ratio (the ratio of the feed rate of H_2 to the feed rate of CO) at the cost of a higher CO_2 selectivity [3]. Iron also provides greater resistance to poisoning by sulfur, but inferior resistance to coking and attrition [3]. Iron gives a more olefinic product and suppressed methane formation [4].

Sasol's original LTFT reactor design utilized a fixed bed, as does a shell design [5]. This form of operation is Gas Phase Fischer Tropsch (GP-FTS). To overcome the limitations of GP-FTS (poor extraction of products and heat from the catalyst, high pressure drop, and poor economies of scale), Sasol developed their slurry bed reactor (SP-FTS) [5]. Kaoru Fujimoto's group [6] pioneered the use of a supercritical fluid as the reaction medium for fixed bed LTFT (SC-FTS) to mitigate some of the problems seen in GP-FTS. A number of benefits have been seen in SC-FTS relative to GP-FTS, including suppressed methane formation [6–12], CO_2 formation [8,12] and improved activity maintenance [10]. Additionally, many researchers have seen an enhancement in the olefin selectivity into higher carbon numbers [8,9,12–15]. This can be explained by the supercritical media having a high capacity to extract and stabilize products that would otherwise undergo secondary reactions (such as olefin hydrogenation to paraffins).

The mechanism of the Fischer Tropsch reaction is still a matter of contention, with Claeys and van Steen listing four pathways [16]: the alkyl mechanism, the alkenyl mechanism (associated with Maitlis), the enol mechanism (associated with Storch), and the CO insertion mechanism (via coordination chemistry and homogenous catalysis). Three key aspects of any Fischer Tropsch Mechanism are: (1) the pathway for CO dissociation (whether it is unassisted – prior to hydrogenation. or assisted – after some hydrogenation), (2) the structure of the initiator species, and (3) the structure of the propagator species. See Table 1 for a presentation of the four mechanisms listed above.

For non-oxygenate mechanisms, the formation of oxygenates is often explained as being due to a different termination step, usually CO insertion [4,16,17]. In preliminary work, we observed a significant selectivity to diesel-length aldehydes on an iron–zinc catalyst promoted with copper and potassium. The remainder of this study was undertaken to determine the role of these products in the reaction pathway.

* Corresponding author. Tel.: +1 334 844 2036; fax: +1 334 844 2063.
E-mail address: croberts@eng.auburn.edu (C. Roberts).

0926-860X/$ – see front matter © 2010 Elsevier B.V. All rights reserved.
doi:10.1016/j.apcata.2010.07.032

Table 1
Role of hydrogen in CO dissociation, initiator, and propagator for four proposed FTS mechanisms. Information from Ref. [16].

Mechanism	Alkyl	Alkenyl	Enol	CO insertion
CO Dissociation	Unassisted	Unassisted	Assisted	Assisted
Initiator	RCH_2	RCHCH	RCOH or RCHOH	RCH_2
Propagator	CH_2	CH_2	CHOH	CO

2. Experimental

2.1. Catalyst synthesis

Three batches of catalyst were made and used in this study (all compositions are molar):

A 1.0 Fe:0.10 Zn:0.02 K:0.01 Cu
B 1.0 Fe:0.10 Zn:0.02 K:0.01 Cu
C 1.0 Fe:0.01 Cu:0.02 K

The batches were synthesized by a procedure similar to one published by Enrique Iglesia's group [18]. The materials for this procedure are as follows (all listed here and elsewhere used as received):

Water: DIUF Water (Fisher W2-4).
Ethanol: Absolute Ethyl Alcohol (Pharmco-Aaper E200).
INH: ACS Reagent Grade Iron (III) Nitrate Nonahydrate (Sigma–Aldrich 216828-500G).
ZNH: Reagent Grade Zinc Nitrate Hexahydrate (Sigma–Aldrich 228737-100G).
AC: ACS Reagent Grade Ammonium Carbonate (Sigma–Aldrich 207861-500G).
CNH: ACS Reagent Grade Copper (II) Nitrate Hydrate (Sigma–Aldrich 223395-100G).
PC: ACS Reagent Grade Potassium Carbonate (Sigma–Aldrich 209619-100G).

For each batch, a stock iron solution (1 M INH and 0.1 M ZNH in water for Batch A and Batch B, 1 M INH for Batch C) and a stock reducing solution (AC in water – saturated at room temperature) were made.

At a controlled rate (2 mL/min for Batches A and Batch C, 6 mL/min for Batch B), the iron solution was added to water (50 mL for Batch A and Batch C, 150 mL for Batch B) maintained at 80 °C using an Eldex Laboratories Syringe Pump (B-100-S). The reducing solution was added manually to maintain the pH at 7.0 (as measured by a Denver Instrument UB-10 pH meter) with vigorous stirring (via magnetic stir bar). At the end of the co-precipitation (15 min for Batch A, 45 min for Batch B, 90 min for Batch C), reagent addition was stopped and the solution allowed to cool with continued stirring. The slurry was then vacuum filtered. The filter cake was re-slurried in water and then re-filtered 4 times. The filter cake was then re-slurried in ethanol and then vacuum filtered twice. The filter cake was then dried overnight at 80 °C.

The dried catalyst was then calcined at atmospheric pressure in flowing air, the temperature ramped at 5 °C/min and held at 400 °C for 240 min. When the catalyst had cooled, the pore volume was determined by the addition of water (measured by mass). The catalyst was then dried again at 80 °C.

The potassium (PC) and copper (CNH) promotion were done by incipient wetness impregnation, with the catalyst dried overnight at 80 °C and calcined in flowing air with the temperature ramped at 5 °C/min to 400 °C and held for 4 h after each impregnation. For Batch A and Batch B, the potassium impregnation was done prior to copper impregnation. For Batch C, the copper impregnation was done first.

For every experiment, the calcined catalyst was activated (reduced) in situ using syngas (50 SCCM/g) at 270 °C.

2.2. Apparatus

Two reactor systems were used in this study: a fixed bed reactor for GP-FTS and SC-FTS and a stirred Parr Reactor for SP-FTS.

A schematic of the fixed bed reactor system is shown in Fig. 1. In this system, syngas (A) and helium (B, when appropriate) are fed through a mass flow controller (C) and mixed with hexanes (D, for SC-FTS) fed through a positive displacement HPLC pump (E). The mixture passes through heated lines to the reactor (F, downflow) in a split tube furnace (G). From the reactor, the effluent passes through heated tubing to the hot trap (H, maintained at 200 °C to condense heavy wax, ideally without significant partitioning below C20). The hot trap condensate is allowed to accumulate and can be periodically collected and analyzed. The vapor from the hot trap passes through heated tubing to the BPR (I, back pressure regulator, used to maintain the reactor pressure), and through heated tubing to the cold trap (J, maintained at slightly sub-ambient temperature). Liquids are allowed to accumulate in the cold trap and are periodically collected and analyzed via manual injection to the FID-GC. The gasses from the cold trap pass to a six-way injection valve (K) used to automatically inject them to the TCD-GC. From there the gasses are vented to the fume hood.

The reactor in this system is an HIP microreactor with a length of 10 inches and an ID of 0.5 in. The upper half has been reamed out to an ID of 0.625 in. A stainless steel filter disk rests on the rim between the larger and smaller ID sections, with the catalyst resting upon the disk. The thermocouple is a 6-point profile thermocouple (Omega Engineering PP6-36-K-G-18) with the third junction in the catalyst bed and used to control the furnace.

A schematic of the Parr Reactor is shown in Fig. 2. In this system, syngas (A) and helium (B, when appropriate) are fed through a mass flow controller (C), then through a heated line into the reactor (D) where they are bubbled through the agitated (600 RPM) slurry. Vapor is pulled off of the top of the reactor and passes through a heated line to the cold trap (E, maintained at sub-ambient temperature). The condensate in the cold trap is allowed to accumulate to be periodically collected and analyzed by manual injection to the FID-GC. The vapor from the cold trap passes through a BPR (F, used to maintain the reactor at the desired pressure), then the 6-way valve (G, used to automatically inject to the TCD-GC), and finally is vented to the fume hood. Positioning the BPR after the cold trap creates some analytical problems (loss of light products during liquid collection), but improves the reliability of the system. The reactor was pre-filled with 500 mL of wax which was slurried with 4 g of iron catalyst.

The syngas was purchased pre-mixed from Airgas (Certified Standard) with 1.5% N_2 (internal standard) and $H_2/CO = 1.65$. The helium is UHP grade and is used for pressure testing, startup, and shut-down. The hexanes (the media used during SC-FTS) was purchased in bulk from Fisher Scientific. The paraffin wax (the media used during SP-FTS) was purchased from Fisher Scientific (CAS 8042-47-5). It is a complex mixture of unknown components that elutes from the FID-GC between the C22 and C35 n-paraffins.

Analysis of the cold trap vapor stream was done by online injection (Valco 6-way valve) to a Varian 3800 GC with a TCD detector

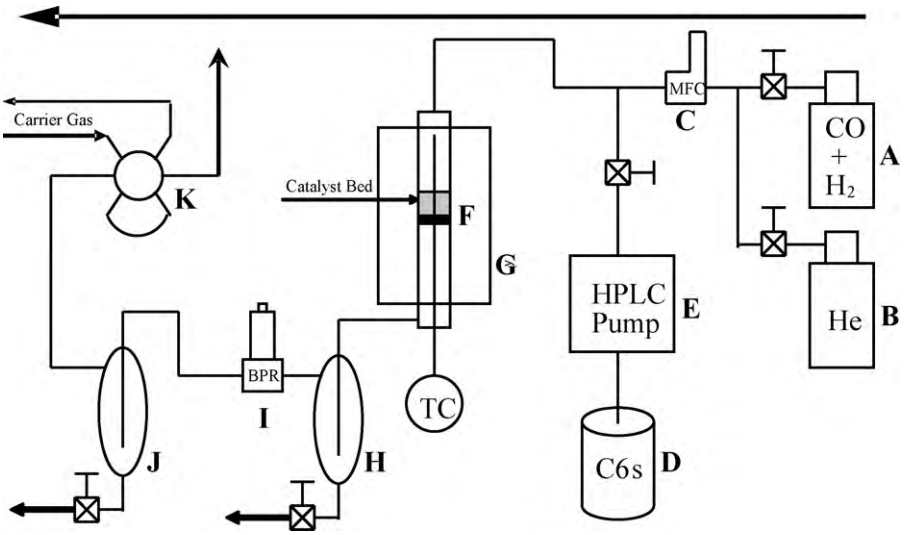

Fig. 1. Schematic of the fixed bed reactor system (used for GP-FTS and SC-FTS). (A) Syngas cylinder, (B) helium cylinder, (C) mass flow controller, (D) hexanes bottle, (E) HPLC pump, (F) reactor, (G) furnace, (H) hot trap, (I) BPR, (J) cold trap, (K) 6-way valve.

and a Hayesep column (Grace Davison 2836PC). Standards were used to determine the response factors of the various components and the N_2 internal standard was used to determine the rate of the cold trap vapor stream. Analysis of the cold trap liquids and Parr reactor residual liquids was done by manual injection to a Varian 3300 GC with an FID detector and a DB-5 column (Agilent 125-5032). The mass response factors were assumed to be identical for all pure hydrocarbon components (olefins, paraffins, and isomers) and determined by standard injection for other classes of products (alcohols and aldehydes).

The GC/MS analysis was performed at the Auburn University Mass Spec Center. The analysis utilized a Waters 6890N GC with a DB5-MS column (Cat# 1225532, J&W Scientific) coupled to a Time of Flight Mass Analyzer (GCT Premier, Waters). Component identification was done by comparing the electron impact fragmentation pattern (70 eV) with those in the compound library (NIST 2003). Compounds with Match and Reverse Match scores above 800 and probabilities above 90% were selected as matches. The identification was confirmed by elemental composition analysis using accurate mass measurement with an internal calibrant (lock-mass 218.9856 *m*/*z*, heptacosafluorotributylamine, Sigma) with an acceptable error of less than 5 ppm and by isotope modeling comparing the experimental and theoretical isotope distribution. The component identifications from the GC/MS were also confirmed by retention time of standard compounds on the FID-GC. Quantitative analysis was done on the FID-GC with response factors determined though the analysis of corresponding standards.

2.3. Procedure

First study (GP-FTS and SC-FTS study): the first study used 2 g of the Batch A catalyst in the fixed bed reactor system. After a brief (ca. 10 h) period under GP-FTS conditions the system was converted to SC-FTS operation. After a series of system upsets due to mechanical issues, the reactor was stabilized and a brief study was conducted at various syngas rates (150 SCCM syngas, 100 SCCM, 50 SCCM, 300 SCCM, 150 SCCM, sequentially), with the media (hexanes) to syngas ratio kept at 1 mL/min per 50 SCCM (approximately 3.5 mol media per mol syngas). During GP-FTS operation, the pressure was maintained at 17.5 bar. During SC-FTS operation, the pressure was maintained at 75 bar (maintaining the syngas partial pressure at 17.5 bar). With the exception of the catalyst activation (done at

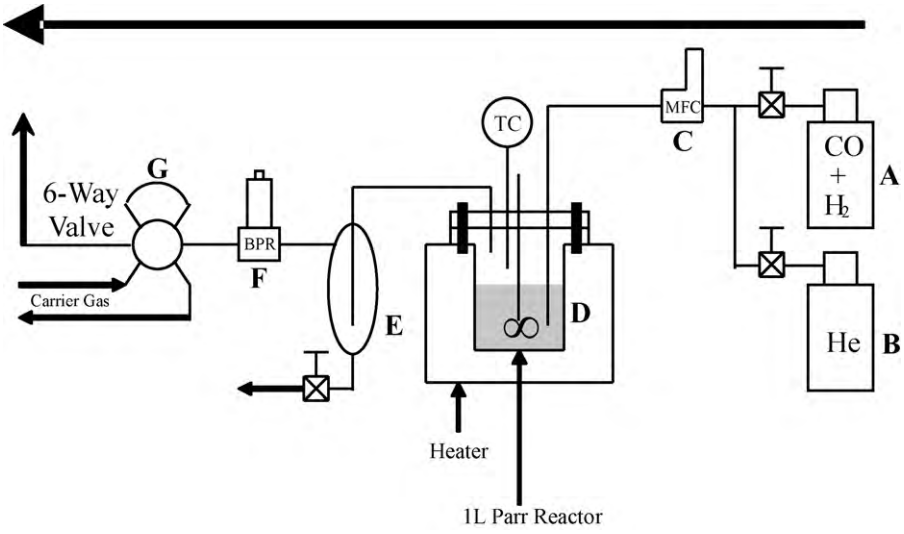

Fig. 2. Schematic of the Parr Reactor (used in the SP- FTS). (A) Syngas cylinder, (B) helium cylinder, (C) mass flow controller, (D) reactor, (E) cold trap, (F) BPR, (G) 6-way valve.

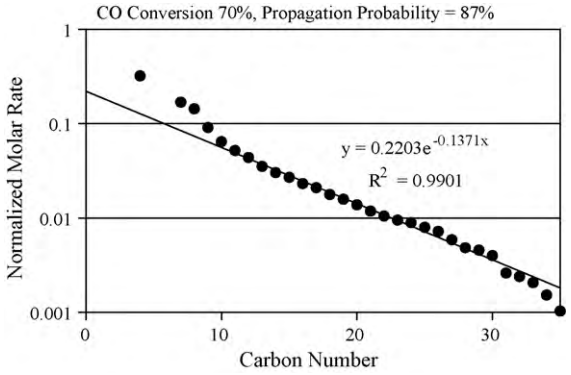

Fig. 3. First study (SC-FTS)—ASF Plot (2 g catalyst, 150 SCCM syngas, 3 mL/min hexanes, P = 75 bar, T = 240 °C, X_{CO} = 70%).

270 °C and 1 bar), the reaction temperature was maintained at 240 °C.

Second study (GP-FTS and SP-FTS comparison): the second study used the Batch B catalyst, testing it both for GP-FTS and SP-FTS. In the GP-FTS study 2 g of catalyst were loaded into the fixed bed reactor. Once conversion had stabilized, the syngas rate was varied (100 SCCM, 200 SCCM, 100 SCCM, 50 SCCM, sequentially) to determine the reactor performance over a broad range of conversion levels over the 150 h time on stream. The experiment was done at 240 °C. For the SP-FTS portion of the second study, the reactor was loaded with 500 mL of paraffin wax and 4 g of catalyst. After the reduction, the reactor was briefly run at double rate (syngas rate = 400 SCCM) and 270 °C, then regular rate (200 SCCM) and 270 °C before going to the regular rate (200 SCCM) and temperature (240 °C). For both the GP-FTS and SP-FTS the pressure was held at 17.5 bar.

Third study (SC-FTS): the third study used the Batch C catalyst, diluting 1 g of catalyst in 10 g of acid washed and calcined silica sand (Acros Organics 370940010) under SC-FTS conditions. After allowing the system performance to stabilize, the syngas rate was varied: 100 SCCM, 50 SCCM, 100 SCCM, 200 SCCM, then 100 SCCM to test selectivity at moderate, high, and low conversion levels (the hexanes rate was maintained at 1 mL/min/50 SCCM). After the study of the selectivity at different conversion levels, the incorporation of aldehydes, alcohols, and olefins were studied.

In the incorporation portion of this study, the system was first run under normal SC-FTS conditions to give a baseline. The media was then doped with octyl aldehyde (Acros Organics 129481000). After returning to baseline, fresh media was doped with octyl alcohol (Aldrich 47232-8). Following another return to baseline, the fresh media was doped with 1-octene (Acros Organics 301250025), and the study concluded with a return to baseline. Each portion of the incorporation half of this study lasted approximately 12 h with each dopant fed at a concentration of 0.20 mol per mol CO. The effects of the attempted incorporation were determined by comparing the conversion and amounts of various products seen during attempted incorporation with that seen during the baseline preceding and following it.

3. Results

3.1. Overall product distribution

The overall product distribution for the first study (SC-FTS – Fig. 3), the second study (GP-FTS – Fig. 4 and SP-FTS – Fig. 5), and the third study (SC-FTS – Fig. 6) are as follows. The slurry-phase ASF plot has the three separate product fractions (cold trap gasses, cold trap liquids, and reactor residual liquids).

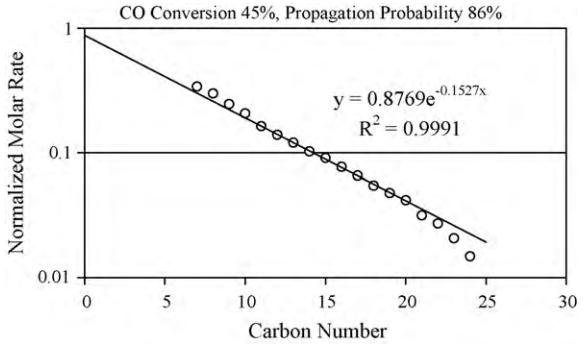

Fig. 4. Second study (GP-FTS)—ASF plot (2 g catalyst, 100 SCCM syngas, P = 17.5 bar, T = 240 °C, X_{CO} = 45%).

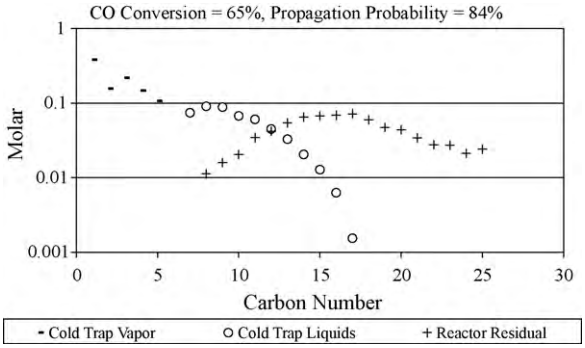

Fig. 5. Second study (SP-FTS)—ASF plots (not normalized) (4 g catalyst, 200 SCCM, P = 17.5 bar, T = 240 °C, X_{CO} = 65% for cold trap vapor and cold trap liquid. Products from whole run for reactor residual).

With the possible exception of GP-FTS, each of the ASF plots shows a 2-alpha distribution with the two regions meeting in the low teens. For this work, the most important observation is that the high-carbon number alpha values are consistent among the different catalyst batches and reaction media. Additionally, the ASF plots for different conversion levels under GP-FTS and SC-FTS are not shown, but there is little influence of conversion level on the ASF plots.

3.2. Gas product analysis

The crossplot of CO_2, CH_4, and C3 olefin selectivity versus CO conversion for the first study is presented in Fig. 7. The CO_2 selectivity is calculated on a CO basis [CO_2 generated/CO consumed], the methane selectivity on a CO_2-free basis [CH_4 generated/(CO consumed − CO_2 generated)], and the C3 olefin selectivity on a C3 hydrocarbon basis [propene/(propene + propane)]. Operation

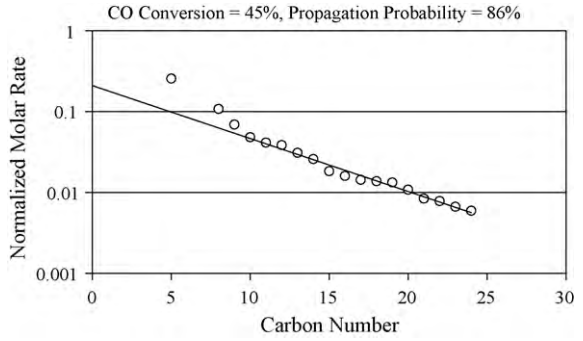

Fig. 6. Third study (SC-FTS)—ASF plot (1 g catalyst, 200 SCCM syngas, 4 mL/min hexanes, P = 75 bar, T = 240 °C, X_{CO} = 45%).

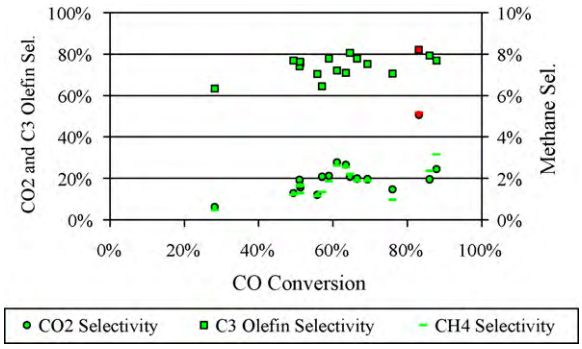

Fig. 7. First study (SC-FTS (empty, green in web) and GP-FTS (shaded, red in web))—CO_2, C3 Olefin, and CH_4 vs. CO Conversion.

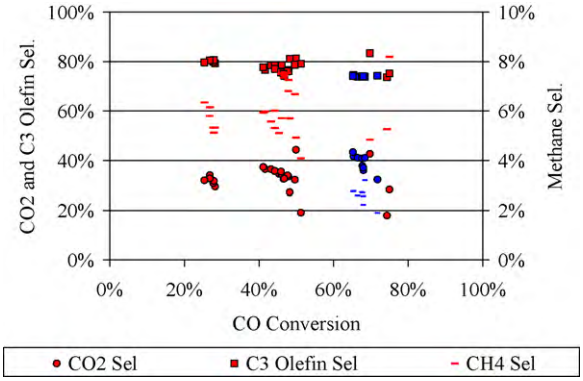

Fig. 8. Second study (GP-FTS (empty, red in web) and SP-FTS (full, blue in web))—CO_2, C3 Olefin, and CH_4 vs. CO Conversion.

under SC-FTS conditions suppressed the methane and CO_2 selectivity significantly and the C3 olefin selectivity slightly relative to GP-FTS. The methane and CO_2 selectivity both decreased markedly with decreasing CO conversion, appearing to extrapolate to zero as the CO conversion approaches zero and the product distribution becomes the primary product distribution. Additionally, the C3 olefin selectivity appeared to drop as the CO conversion decreased, though not appearing to extrapolate to zero as CO conversion approached zero, indicating that propene is likely both a primary and secondary product.

The crossplot of CO_2, CH_4, and C3 olefin selectivity versus CO conversion for the second study is presented in Fig. 8. Under GP-FTS operation, there was no trend in CO_2, CH_4, or C3 olefin selectivity versus CO conversion. Going from GP-FTS to SP-FTS gave a mild suppression in C3 olefin selectivity, a mild increase in CO_2 selectivity,

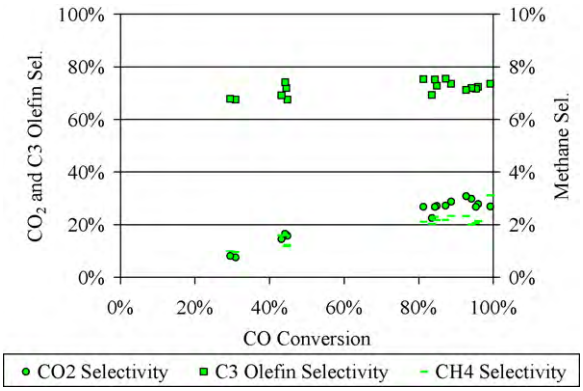

Fig. 9. Third study (SC-FTS)—CO_2, C3 Olefin, and CH_4 vs. CO Conversion.

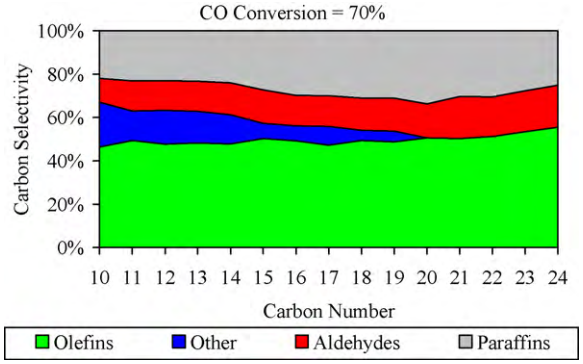

Fig. 10. First study (SC-FTS)—breakdown of liquid product by type –v– carbon number (2 g catalyst, 150 SCCM syngas, 3 mL/min hexanes, P = 75 bar, T = 240 °C, X_{CO} = 70%, propagation probability = 87%).

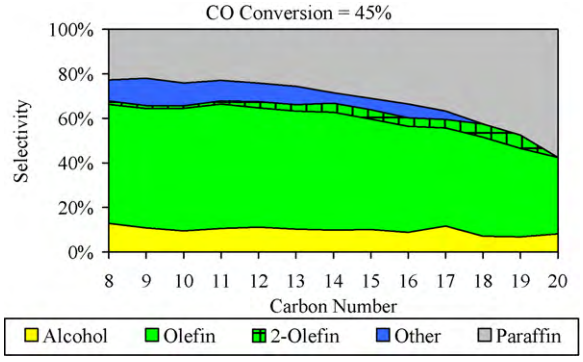

Fig. 11. Second study (GP-FTS)—breakdown of liquid product by type –v– carbon number (2 g catalyst, 100 SCCM syngas, P = 17.5 bar, T = 240 °C, X_{CO} = 45%, propagation probability = 86%).

and a large decrease in CH_4 selectivity. The decrease in methane selectivity in going from GP-FTS to SP-FTS is comparable to that seen in going from GP-FTS to SC-FTS.

The crossplot of CO_2, CH_4, and C3 olefin selectivity versus CO conversion for the third study is presented in Fig. 9. The SC-FTS results seen in this study (with a zinc-free catalyst) match those seen in SC-FTS operation in the first study. Methane and CO_2 again appear to be secondary products while propene appears to be both a primary and secondary product.

3.3. Liquid product breakdown by type

The breakdown of the liquid product by type versus carbon number for the first study during SC-FTS operation is shown in Fig. 10 (the same liquid sample used to generate the ASF plot shown in Fig. 3). With the exception of the "Other" products gradually disappearing, there is little influence of carbon number on the relative amounts of olefins, paraffins, and aldehydes (the aldehyde identification was confirmed by GC retention time and GC–MS analysis). The analytical procedure used in this study lumped the alcohols into the "Other" category. Branching has been shown to decrease with increasing carbon number [4].

The breakdown of the liquid product by type versus carbon number for the second study is shown in Fig. 11 (GP-FTS operation – the same sample used for the ASF plot in Fig. 4) and Fig. 12 (SP-FTS operation cold trap liquids – the same liquid sample used for the ASF plot in Fig. 5).

The GP-FTS breakdown showed different behavior than that seen in Fig. 10 with SC-FTS. First, the liquid aldehydes were not present in GP-FTS in detectable quantities while internal olefins were observed. Second, with increasing carbon number the GP-FTS

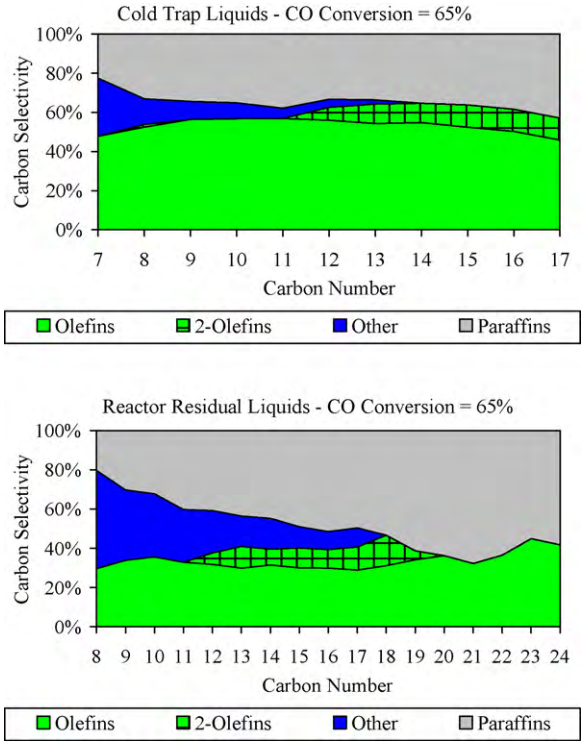

Fig. 12. Second study (SP-FTS)—breakdown of liquid product by type –v– carbon number (4 g catalyst, 200 SCCM syngas, P = 17.5 bar, T = 240 °C, X_{CO} = 65%, propagation probability = 84%).

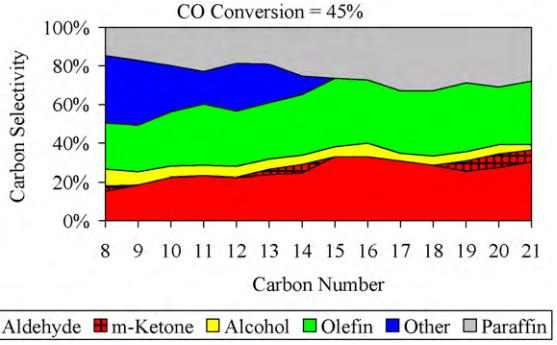

Fig. 13. Third study (SC-FTS)—breakdown of liquid product by type –v– carbon number (1 g catalyst, 200 SCCM syngas, 4 mL/min hexanes, P = 75 bar, T = 240 °C, X_{CO} = 45%, propagation probability = 86%).

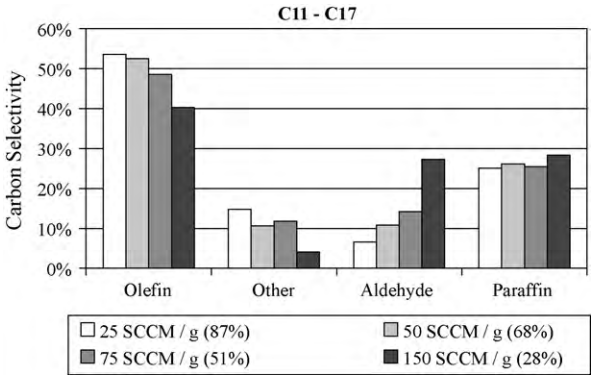

Fig. 14. First study (SC-FTS)—breakdown of liquid product by type –v– conversion level (P = 75 bar, T = 240 °C, CO conversion in parenthesis).

liquid product became much less olefinic and more paraffinic, indicating the hydrogenation of olefins to their corresponding paraffins.

The SP-FTS product breakdown by type, like that in the first study, did not isolate alcohols from the "Other" category. As with GP-FTS, no liquid aldehydes were seen in this SP-FTS study while significant quantities of internal olefins were detected. Like SC-FTS, the product distributions in the cold trap liquids and reactor residual liquids were independent of carbon number, apart from the gradual disappearance of the "Other" products. The cold trap liquids in SP-FTS were far more olefinic than the reactor residual liquids, which is consistent with the reactor residual liquids having a far higher contact time. A greater fraction of the reactor residual liquids are present as "Other" products than in the cold trap liquids. Assuming that these products are predominately branched products, the higher selectivity in the reactor residual liquids supports branched compounds as secondary products, likely formed from olefins. The apparent disappearance of internal olefins at the end of the diesel range is due to analytical limitations at the corresponding high retention times for these compounds.

The breakdown of liquid product by type versus carbon number for SC-FTS on a zinc-free iron catalyst from the third study is shown in Fig. 13. This SC-FTS study gave very similar results to those obtained from the first SC-FTS study (Fig. 10), with little change versus carbon number apart from the gradual disappearance of "Other" products. It is important to note that the analytical procedures employed during the third study were improved to allow for the detection of alcohols and methyl-ketones (the methyl-ketone identification was confirmed by GC retention time and GC–MS analysis). As in the first study, significant quantities of liquid aldehydes were detected in this SC-FTS investigation. A significant quantity of methyl-ketones was also found.

In Fig. 13, it appears that methyl-ketones are only present at C8, from C13 to C14, and >C18. However, this sporadic appearance is due to analytical limitations. The methyl-ketones retention time is similar to that of the paraffin of two greater carbon number. At a low carbon number (C8), the methyl-ketone elutes prior to the olefin. At higher carbon numbers (C9–C12) the methyl-ketone is indistinguishable from the olefin. The methyl-ketone can again be observed from C13 to C14 between the paraffin and the olefin. The methyl-ketone peak then merges with the paraffin peak from C15 to C18. Above C19 the methyl-ketone elutes after the paraffin and is observed until it disappears into signal noise. It is prohibitively likely that the methyl-ketones are present at the carbon numbers where the peak cannot be resolved with selectivities similar to the carbon numbers where they are resolvable.

The breakdown of the liquid products by type versus conversion level for the first study under SC-FTS conditions is shown in Fig. 14 with the analysis limited to the C11–C17 range. As CO conversion decreased and the product spectrum approached the primary product spectrum, the aldehyde selectivity increased markedly while the "Other" and olefin selectivity decreased. The paraffin selectivity was largely unaffected by conversion level. This indicates that aldehydes are primary products. The "Other" products appear to be secondary products. The olefins appear to be secondary products as well, but it is doubtful that the olefin selectivity would go to zero if the CO conversion was extrapolated to zero, indicating that olefins are both primary and secondary products. Paraffins appear to be primary products, and the hydrogenation of olefins to paraffins appears to be effectively suppressed under supercritical conditions, as evidenced by the lack of an increase in paraffinicity with increasing carbon number (Fig. 10) or increasing CO conversion (Fig. 14).

The breakdown of the liquid products by type versus conversion level for the second study under GP-FTS conditions is shown in Fig. 15 for the C10–C17 range. With decreasing CO conversion, here the product becomes less paraffinic and more olefinic. This sup-

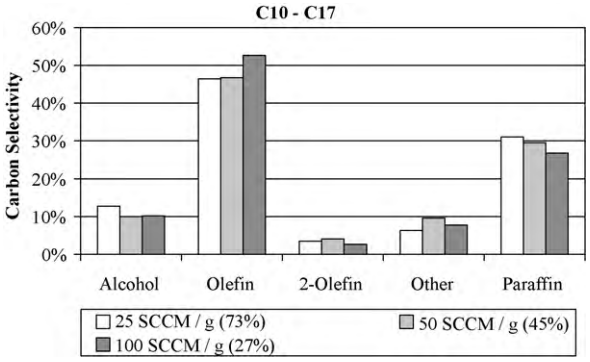

Fig. 15. Second study (GP-FTS)—breakdown of liquid product by type –v– conversion level (P = 17.5 bar, T = 240 °C, CO conversion in parenthesis).

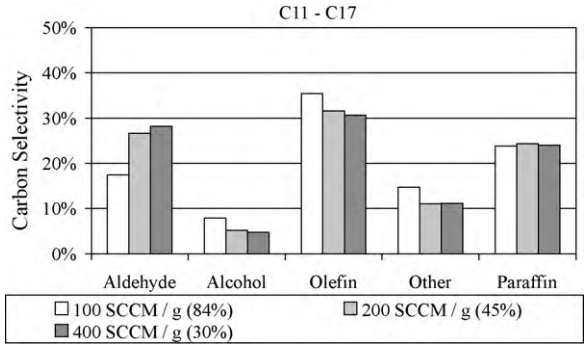

Fig. 16. Third study (SC-FTS)—breakdown of liquid product by type –v– conversion level (P = 75 bar, T = 240 °C, CO conversion in parenthesis).

ports olefins as primary products that are converted by secondary reactions to paraffins, contrary to what was seen in SC-FTS operation. We believe this to be due to the failure the GP-FTS media to inhibit the consumption of the aldehyde or aldehyde-like reaction intermediate. Consequently, because the consumption of aldehydes is nearly complete even at low conversion levels in GP-FTS, with increasing CO conversion the secondary reaction that is observed is the hydrogenation of the olefins giving a false view of the primary product spectrum.

The breakdown of the liquid products by type versus conversion level for the third study under SC-FTS conditions is shown in Fig. 16 for the C11–C17 range. This data confirms much of what was seen in the first study in SC-FTS (Fig. 14) while adding additional information, with aldehydes appearing to be primary products that are converted via secondary reactions to alcohols and olefins. It appears that olefins would have a significant selectivity even with a CO conversion approaching 0%, making it likely that they are both primary and secondary products. Paraffins appear to be primary products and their formation through secondary reactions appears to be suppressed.

The breakdown of the liquid products by type versus conversion level for the third study under SC-FTS conditions is shown in Fig. 17 for the C20–C24 range. While "Other" products are no longer distinguishable from the chromatogram noise and the alcohol peak can no longer be distinguished from the olefin peak, the olefin, paraffin, methyl-ketone, and aldehyde peaks are still distinguishable. This data again confirms aldehydes as primary products that are partially converted to olefins, olefins as both primary and secondary products, methyl-ketones as likely secondary products, and paraffins as primary products.

The observations reported here for SC-FTS have been replicated in our laboratory multiple times, but, for simplicity, only selected experiments are reported here. The same results (i.e., significant

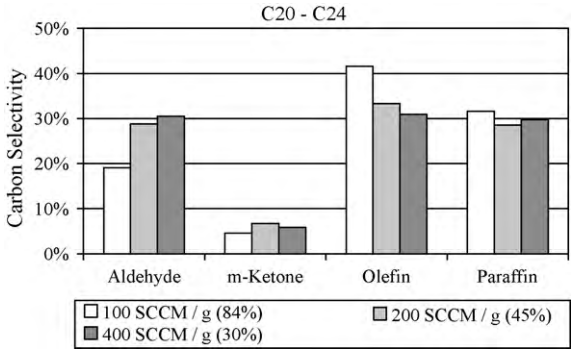

Fig. 17. Third study (SC-FTS)—breakdown of liquid product by type –v– conversion level (P = 75 bar, T = 240 °C, CO conversion in parenthesis).

selectivity to liquid aldehydes, minimal influence of carbon number on the product type breakdown, an increase in aldehyde selectivity with decreasing CO conversion, a decrease in olefin selectivity with decreasing CO conversion, and no influence of CO conversion on the paraffin selectivity) were obtained in another SC-FTS study using a 1 Fe:0.1 Zn:0.01 Cu:0.02 K by mol catalyst and another study using Batch C without a hot trap in the reactor system.

3.4. Aldehyde, alcohol, and olefin incorporation

After the completion of the third study presented above, an additional investigation was undertaken to explore the incorporation of added C8 aldehyde, C8 alcohol, and 1-octene in the Fischer Tropsch reaction. The incorporant was added to the hexanes media such that it was present at the reactor inlet at a rate 20% of that of the CO in the syngas. The analysis was performed by comparing the performance during the attempted incorporation (conversion of CO and H_2 and the production rate of the different products) with that observed during a period of SC-FTS operation without an incorporant immediately preceding and following the attempted incorporation. C8 aldehyde incorporation was studied first, followed by C8 alcohol incorporation, and finally 1-octene incorporation.

The addition of the C8 aldehyde resulted in some incorporation into heavier products with a selectivity comparable to that seen in the baselines (i.e. no incorporant added). There was no distinguishable effect of the C8 aldehyde on conversion, methane selectivity, or CO_2 selectivity. The formation of C2 and C3 products appear to have been suppressed. In addition to incorporation, the C8 aldehyde was converted to the C7 paraffin, C8 olefin, C8 alcohol, C9 methyl-ketone, C9 alcohol, and an unknown C15 oxygenate.

The addition of the C8 alcohol resulted in some incorporation into heavier products with a selectivity comparable to that seen in the baselines. There was no distinguishable effect of the C8 alcohol on conversion, methane selectivity, CO_2 selectivity, C2 selectivity, or C3 selectivity. In addition to the incorporation, the C8 alcohol appears to have been converted to the C8 aldehyde, C9 alcohol, and C9 aldehyde.

The addition of 1-octene resulted in no discernible incorporation into heavier products. There was no change in CO conversion, though a drop in usage ratio was observed. The methane, CO_2, C2 and C3 selectivities were unchanged. The 1-octene was converted to C8 internal olefins, the C8 paraffin, and a product that is likely the C10 olefin.

4. Discussion

Low temperature Fischer Tropsch produces two classes of products: hydrocarbons and oxygenates. The predominant hydrocarbon products are n-paraffins, n-olefins (mostly terminal), and branched

paraffins and olefins. Minor hydrocarbon products include aromatics and dienes. The predominant oxygenates are aldehydes (mostly linear), alcohols (mostly terminal and linear), ketones (with the carbonyl group mainly on the β-carbon), carboxylic acids (mostly linear), and esters (mostly linear). Minor oxygenate products include acetals, ethers, furans, and phenols [19].

Paraffins are shown to be primary products by varying the residence time (conversion level) under SC-FTS conditions. There are several possible pathways for their formation. Burt Davis' group observed the conversion of added alcohols to the one carbon shorter paraffin in a process that also formed CO_2 [20] in a slurry-phase reactor. However, under SC-FTS conditions, we did not observe the formation of the one shorter paraffin from an added alcohol, but did observe this phenomenon with the added aldehyde. The conversion of the aldehydic intermediate to a 1-carbon shorter paraffin is a possible pathway to the primary formation of paraffins. However, the apparent absence of CO_2 as a primary product, the absence of methane as a primary product, and the absence of heavier paraffins as secondary products make us consider this unlikely. As such, we prefer the alpha-hydrogenation of a surface alkyl group as a more plausible mechanism for the primary production of paraffins.

The selectivity to diesel-length olefins decreased with decreasing conversion under SC-FTS conditions, contrary to what was seen on the same catalyst under GP-FTS conditions and to what we have observed previously in SC-FTS on a cobalt catalyst. The conversion of octyl aldehyde to 1-octene was observed in the incorporation study, confirming the conversion of aldehydes to olefins as evidenced by the changes is selectivity with variations in conversion. However, the olefin selectivity does not appear to approach zero as CO conversion extrapolates to zero, suggesting that olefins are also primary products. Beta hydrogen elimination from a surface alkyl group is a plausible mechanism for the primary production of olefins. No discernable internal olefins were detected under SC-FTS operation, though internal olefins were seen in GP-FTS and SP-FTS, supporting internal olefins as only secondary products. Additionally, 1-octene, when added to SC-FTS, did form some internal octenes, supporting this conclusion.

Branched compounds have been shown to be formed from the incorporation of non-terminal alcohols [20]. The high selectivity to 'Other' products (presumed to be predominantly branched compounds) in the reactor residual liquids in SP-FTS also suggests their formation from olefins. While the incorporation of 1-octene was not seen in this work, it has been generally observed, albeit at a lower rate than that for alcohols [20]. A terminal olefin should allow for initiation at the 1 carbon (giving an n-paraffin) or 2 carbon (giving a methyl-branched product). A 2-olefin should allow for initiation at the 2 carbon (giving a methyl-branched product) or the 3 carbon (giving an ethyl-branched compound). The formation of methyl-ketones from aldehydes offers a pathway beside isomerization to get from a terminal species to a methyl-branched one. However, under supercritical conditions methyl-ketones are present at carbon numbers into the wax product range while branched products die out in the diesel range.

Aldehydes are demonstrated to be primary products by varying the residence time in SC-FTS. The incorporation study demonstrated their capacity to incorporate into heavier products. Burt Davis' group has shown that incorporated alcohols act as chain initiators [20]; we believe that this is likely to also be the means of incorporation for aldehydes. Aldehydes have elsewhere been shown to give incorporation behavior comparable to that of alcohols [21]. Aldehydes and alcohols appeared to interconvert in the incorporation study, suggesting that either could be the primary and either the secondary product. To study this uncertainty, a simulation was done in AspenPlus using the Peng Robinson equation of state. In this simulation, a stream of hexane, hydrogen, water, octyl aldehyde, 1-octyl alcohol, and 1-octene were fed to an equilibrium reactor at typical SC-FTS conditions (P = 75 bar, T = 240 °C) where the aldehyde, alcohol, and olefin were free to be interconverted to minimize the Gibbs Free Energy of the system. The results of this simulation are shown in Table 2. The simulation indicates that the conversion of aldehydes to alcohols and alcohols to olefins should be, under typical SC-FTS conditions, near total. Consequently, given the high ratio of aldehydes to alcohols observed, we conclude that aldehydes are primary over alcohols. The fact that added 1-octene did not react to give an aldehyde further establishes that the aldehydes are not secondary products of olefins, but that the reverse is true. Additionally, in 1962, Wender [22] demonstrated that the synthesis of an aldehyde from an olefin of one fewer carbon number with cobalt hydrocarbonyls readily occurs.

Table 2
Simulation of the thermodynamics of aldehyde, alcohol, and olefin inter-conversion at SC-FTS conditions.

	Feed (mol/h)	Product (mol/h)
Hexane	3.5	3.5
Hydrogen	0.25	0.24
Water	0.25	0.27
Octyl aldehyde	0.01	4.5×10^{-7}
1-Octyl alcohol	0.01	6.1×10^{-5}
1-Octene	0.01	0.030

Alcohols are likely secondary products from the hydrogenation of aldehydes given the two products' capacity for inter-conversion, the drop in alcohol selectivity with decreasing CO conversion, and their capacity to be converted to heavier products.

Methyl-ketones appear to be secondary products formed from aldehydes, though they have been asserted to be formed via carboxylic acid decomposition [19]. The pseudo-dimerization product of the added C8 aldehyde to a C15 oxygenate may be a ketone, but it is not a methyl-ketone [23].

Our analytical system does not allow for the detection of carboxylic acids or esters. The inability to measure carboxylic acids is particularly unfortunate since formate-type species have been proposed as being the chain initiator on iron [20].

The high selectivity to aldehydes suggests an oxygenate mechanism (likely CO Insertion [4,16,17]) as, if nothing more, a termination mechanism for the reaction. However, the capacity for an aldehyde to be converted to possibly all of the reaction product types suggests a broader role for CO insertion. The fact that the aldehyde can also initiate chain growth suggests the oxygenate process as the growth mechanism for the reaction as well. The broad spectrum of apparent primary products suggests that there are multiple types of surface species. However, the consistency of the product type with carbon number suggests sequential termination pathways as opposed to parallel mechanisms. As such, we believe the initiator to be fundamentally different from the intermediate (the product of the initiator reacting with the propagator). The specific identity of these two species is still a matter of inquiry. We believe a CO Insertion mechanism to be more likely given the product spectrum than an enol mechanism. Several variations on CO insertion have been proposed [24].

The mechanism for CO dissociation in Fischer Tropsch Synthesis is still a matter of dispute. However, we believe that the case for hydrogen assisted dissociation has been compellingly made [25–27]. Additionally, if hydrogen assisted dissociation is accepted, an oxygenate mechanism in general and CO insertion specifically becomes highly plausible (see Fig. 18).

A C14 labeling incorporation study would be very useful to bring clarity here. Enrique Iglesia's group [17] has made a very strong case that the behavior of an added incorporant does not necessarily match that of the same component produced in situ. Our group has carried out a number of investigations [9,10,12,28] of SC-FTS on a cobalt catalyst and we have not observed diesel-length aldehydes.

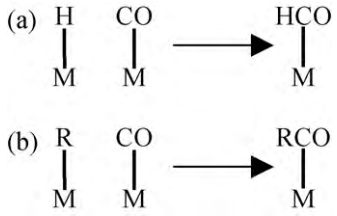

Fig. 18. Presentation of (a) the hydrogenation of CO prior to dissociation (hydrogen assisted dissociation) and (b) CO Insertion. No claim as to the nature of the bond between the CO and the catalyst is intended.

There are two possibilities here. The first is that cobalt-based FTS has a different mechanism that would not produce aldehydes as primary products. The second is that, even if cobalt-based FTS utilizes the same mechanism as iron, cobalt is a much stronger hydrogenation catalyst than iron [29], so the aldehydes would be too rapidly converted to olefins and paraffins to be observed at higher carbon numbers. As such, while we feel based on the data presented here that CO insertion in some form is the chain growth mechanism for FTS on an iron catalyst, we cannot make any claims for cobalt.

5. Conclusions

We have used an iron-based FT catalyst (1 Fe:0.1 Zn:0.02 K:0.01 Cu by mol) for Fischer Tropsch Synthesis in a supercritical (SC-FTS), gas phase (GP-FTS), and slurry-phase (SP-FTS) environment. In SC-FTS, a significant selectivity in the diesel range to aldehydes and methyl-ketones was observed (both products confirmed by GC-MS). These products were not detected under GP-FTS or SP-FTS operation. Additionally, another iron-based FT catalyst (1 Fe:0.01 Cu:0.02 K by mol) was studied under SC-FTS conditions and similar products were observed. We attribute this to the supercritical media having a high capacity to extract and stabilize products, inhibiting secondary reactions. Decreasing the residence time of the reaction (decreasing conversion to make the product spectrum more primary) gave increased aldehyde and decreased olefin selectivity. From this, we conclude that the aldehydes are primary products and are converted by secondary reactions to olefins. Doping the supercritical media with octyl aldehyde resulted in the aldehyde being incorporated into heavier products, indicating that the process that forms the aldehyde is part of the propagation mechanism. From this, we have concluded that CO Insertion is a likely mechanism for the FTS reaction on iron-based catalysts.

Acknowledgements

The authors would like to gratefully acknowledge financial support from the U.S. Department of Energy National Energy Technology Lab and the U.S. Army TACOM through the Consortium for Fossil Fuel Science, and the Sun Grant Consortium. We would like to express gratitude to Dr. Yonnie Wu, Director of the Auburn University Mass Spec Center, for invaluable assistance in performing the GC/MS experiments and the interpretation of their results. Additionally, we would like to thank Brian Schweiker and Mike Hornsby for their help with instrumentation and equipment, Mario Eden (Auburn University) for his assistance with the Aspen simulation, Mohindar Seehra (West Virginia University) for catalyst characterization, and Enrique Iglesia (University of California at Berkeley) and Andre Steynberg (Sasol) for technical correspondence on specific questions.

Appendix A. Supplementary data

Supplementary data associated with this article can be found, in the online version, at doi:10.1016/j.apcata.2010.07.032.

References

[1] M.E. Dry, Catal. Today 71 (2002) 227–241.
[2] F. Morales, B.M. Weckhuysen, Catalysis 19 (2006) 1–40.
[3] A.Y. Khodakov, W. Chu, P. Fongarland, Chem. Rev. 107 (2007) 1692–1744.
[4] M.E. Dry, Appl. Catal., A 138 (1996) 319–344.
[5] R.L. Espinoza, A.P. Steynberg, B. Jager, A.C. Vosloo, Appl. Catal., A 186 (1999) 13–26.
[6] K. Yokota, K. Fujimoto, Fuel 68 (1989) 255–256.
[7] S. Yan, L. Fan, Z. Zhang, J. Zhou, K. Fujimoto, Appl. Catal., A 171 (1998) 247–254.
[8] G. Jacobs, K. Chaudhari, D. Sparks, Y. Zhang, B. Shi, R. Spicer, T.K. Das, J. Li, B.H. Davis, Fuel 82 (2003) 1251–1260.
[9] X. Huang, C.B. Roberts, Fuel Process. Technol. 83 (2003) 81–99.
[10] N.O. Elbashir, P. Dutta, A. Manivannan, M.S. Seehra, C.B. Roberts, Appl. Catal., A 285 (2005) 169–180.
[11] H. Tang, H. Liu, X. Yang, Y. Li, J. Chem. Eng. Chin. 22 (2008) 259.
[12] E. Durham, S. Zhang, Christopher B. Roberts, AIChE Annual Meeting (2008): Presentation 678d.
[13] K. Yokota, Y. Hanakata, K. Fujimoto, Fuel 70 (1991) 989–994.
[14] X. Lang, A. Akgerman, D.B. Bukur, Ind. Eng. Chem. Res. 34 (1995) 72–77.
[15] D.B. Bukur, X. Lang, A. Akgerman, Z. Feng, Ind. Eng. Chem. Res. 36 (1997) 2580–2587.
[16] M. Claeys, E. van Steen, In: Andre Steynberg, Mark Dry (Eds.), Studies in Surface Science and Catalysis 152 – Fischer Tropsch Technology, Elsevier Science, 2004, pp. 601–680.
[17] P. Enrique Iglesia, Catal. A 161 (1997) 59–78.
[18] P. Senzi Li, S. Krishnamoorthy, A. Li, G.D. Meitzner, E. Iglesia, J. Catal. 206 (2002) 202–217.
[19] A. de Klerk, Fischer Tropsch Refining. PhD Thesis, University of Pretoria, Pretoria, South Africa, 2008.
[20] B.H. Davis, Catal. Today 141 (2009) 25–33.
[21] W. Keith Hall, R.J. Kokes, P.H. Emmett, J. Am. Chem. Soc. 82 (1960) 1027–1037.
[22] I. Wender, H.W. Sternberg, R.A. Friedel, S.J. Metlin, R.E. Markby, Technical Report (1962) OSTI ID: 7193411.
[23] Y. Wang, B.H. Davis, Appl. Catal., A 180 (1999) 277–285.
[24] M. Zhuo, K. Fei Tan, A. Borgna, M. Saeys, J. Phys. Chem. C 113 (2009) 8357–8365.
[25] G. Blyholder, M. Lawless, Langmuir 7 (1991) 140–141.
[26] O.R. Inderwildi, S.J. Jenkins, D.A. King, J. Phys. Chem. C 112 (2008) 1305–1307.
[27] X. Dai, C. Yu, J. Nat. Gas Chem. 17 (2008) 365–368.
[28] N.O. Elbashir, C.B. Roberts, Ind. Eng. Chem. Res. 44 (2005) 505–521.
[29] M.E. Dry, Appl Catal., A 138 (1996) 319–344.